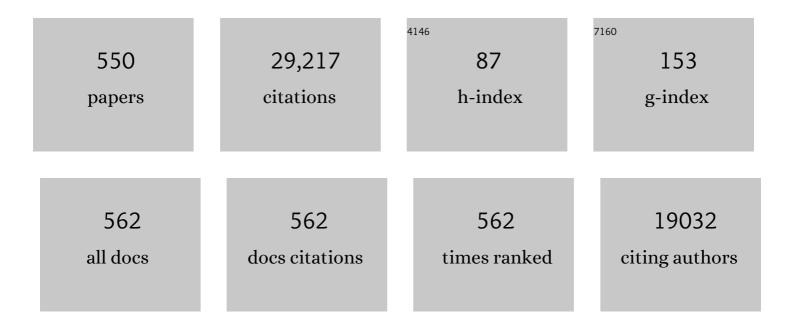
## **Christophe Ballif**

List of Publications by Year in descending order

Source: https://exaly.com/author-pdf/1911281/publications.pdf Version: 2024-02-01



#	Article	IF	CITATIONS
1	Organometallic Halide Perovskites: Sharp Optical Absorption Edge and Its Relation to Photovoltaic Performance. Journal of Physical Chemistry Letters, 2014, 5, 1035-1039.	4.6	2,153
2	Fully textured monolithic perovskite/silicon tandem solar cells with 25.2% power conversion efficiency. Nature Materials, 2018, 17, 820-826.	27.5	1,046
3	High-efficiency Silicon Heterojunction Solar Cells: A Review. Green, 2012, 2, 7-24.	0.4	725
4	Complex Refractive Index Spectra of CH <sub>3</sub> NH <sub>3</sub> PbI <sub>3</sub> Perovskite Thin Films Determined by Spectroscopic Ellipsometry and Spectrophotometry. Journal of Physical Chemistry Letters, 2015, 6, 66-71.	4.6	491
5	Light Trapping in Solar Cells: Can Periodic Beat Random?. ACS Nano, 2012, 6, 2790-2797.	14.6	480
6	Current Losses at the Front of Silicon Heterojunction Solar Cells. IEEE Journal of Photovoltaics, 2012, 2, 7-15.	2.5	479
7	Efficient silicon solar cells with dopant-free asymmetric heterocontacts. Nature Energy, 2016, 1, .	39.5	461
8	Efficient Monolithic Perovskite/Silicon Tandem Solar Cell with Cell Area >1 cm <sup>2</sup> . Journal of Physical Chemistry Letters, 2016, 7, 161-166.	4.6	448
9	Raising the one-sun conversion efficiency of Ill–V/Si solar cells to 32.8% for two junctions andÂ35.9% for three junctions. Nature Energy, 2017, 2, .	39.5	424
10	Silicon heterojunction solar cell with passivated hole selective MoOx contact. Applied Physics Letters, 2014, 104, .	3.3	363
11	22.5% efficient silicon heterojunction solar cell with molybdenum oxide hole collector. Applied Physics Letters, 2015, 107, .	3.3	360
12	Efficient Near-Infrared-Transparent Perovskite Solar Cells Enabling Direct Comparison of 4-Terminal and Monolithic Perovskite/Silicon Tandem Cells. ACS Energy Letters, 2016, 1, 474-480.	17.4	332
13	Perovskite/Silicon Tandem Solar Cells: Marriage of Convenience or True Love Story? – An Overview. Advanced Materials Interfaces, 2018, 5, 1700731.	3.7	321
14	Transparent Electrodes for Efficient Optoelectronics. Advanced Electronic Materials, 2017, 3, 1600529.	5.1	310
15	Organic–inorganic halide perovskite/crystalline silicon four-terminal tandem solar cells. Physical Chemistry Chemical Physics, 2015, 17, 1619-1629.	2.8	308
16	Infrared light management in high-efficiency silicon heterojunction and rear-passivated solar cells. Journal of Applied Physics, 2013, 113, .	2.5	270
17	Nanomoulding of transparent zinc oxide electrodes for efficient light trapping in solar cells. Nature Photonics, 2011, 5, 535-538.	31.4	265
18	Measurement of the Bending Strength of Vaporâ^'Liquidâ^'Solid Grown Silicon Nanowires. Nano Letters, 2006, 6, 622-625.	9.1	258

#	Article	IF	CITATIONS
19	CH_3NH_3PbI_3 perovskite / silicon tandem solar cells: characterization based optical simulations. Optics Express, 2015, 23, A263.	3.4	258
20	Silver thick-film contacts on highly doped n-type silicon emitters: Structural and electronic properties of the interface. Applied Physics Letters, 2003, 82, 1878-1880.	3.3	257
21	Efficient Monolithic Perovskite/Perovskite Tandem Solar Cells. Advanced Energy Materials, 2017, 7, 1602121.	19.5	255
22	Model for a-Si:H/c-Si interface recombination based on the amphoteric nature of silicon dangling bonds. Physical Review B, 2007, 76, .	3.2	238
23	Improved amorphous/crystalline silicon interface passivation by hydrogen plasma treatment. Applied Physics Letters, 2011, 99, .	3.3	238
24	Transition between grain boundary and intragrain scattering transport mechanisms in boron-doped zinc oxide thin films. Applied Physics Letters, 2007, 90, 142107.	3.3	230
25	Sputtered rear electrode with broadband transparency for perovskite solar cells. Solar Energy Materials and Solar Cells, 2015, 141, 407-413.	6.2	223
26	<i>In situ</i> silicon oxide based intermediate reflector for thin-film silicon micromorph solar cells. Applied Physics Letters, 2007, 91, .	3.3	219
27	Highâ€Efficiency Amorphous Silicon Solar Cell on a Periodic Nanocone Back Reflector. Advanced Energy Materials, 2012, 2, 628-633.	19.5	212
28	Raman Spectroscopy of Organic–Inorganic Halide Perovskites. Journal of Physical Chemistry Letters, 2015, 6, 401-406.	4.6	206
29	Opto-electronic properties of rough LP-CVD ZnO:B for use as TCO in thin-film silicon solar cells. Thin Solid Films, 2007, 515, 8558-8561.	1.8	202
30	Damage at hydrogenated amorphous/crystalline silicon interfaces by indium tin oxide overlayer sputtering. Applied Physics Letters, 2012, 101, .	3.3	200
31	Improved Optics in Monolithic Perovskite/Silicon Tandem Solar Cells with a Nanocrystalline Silicon Recombination Junction. Advanced Energy Materials, 2018, 8, 1701609.	19.5	192
32	Relation between substrate surface morphology and microcrystalline silicon solar cell performance. Journal of Non-Crystalline Solids, 2008, 354, 2258-2262.	3.1	190
33	>21% Efficient Silicon Heterojunction Solar Cells on n- and p-Type Wafers Compared. IEEE Journal of Photovoltaics, 2013, 3, 83-89.	2.5	187
34	Plasmonic absorption in textured silver back reflectors of thin film solar cells. Journal of Applied Physics, 2008, 104, .	2.5	185
35	23.5%-efficient silicon heterojunction silicon solar cell using molybdenum oxide as hole-selective contact. Nano Energy, 2020, 70, 104495.	16.0	179
36	High-Bandgap Perovskite Materials for Multijunction Solar Cells. Joule, 2018, 2, 1421-1436.	24.0	173

#	Article	IF	CITATIONS
37	Nanoimprint Lithography for High-Efficiency Thin-Film Silicon Solar Cells. Nano Letters, 2011, 11, 661-665.	9.1	171
38	Stable Dopant-Free Asymmetric Heterocontact Silicon Solar Cells with Efficiencies above 20%. ACS Energy Letters, 2018, 3, 508-513.	17.4	164
39	Building Integrated Photovoltaics (BIPV): Review, Potentials, Barriers and Myths. Green, 2013, 3, .	0.4	160
40	Silicon heterojunction solar cells: Recent technological development and practical aspects - from lab to industry. Solar Energy Materials and Solar Cells, 2018, 187, 140-153.	6.2	159
41	Influence of the substrate geometrical parameters on microcrystalline silicon growth for thin-film solar cells. Solar Energy Materials and Solar Cells, 2009, 93, 1714-1720.	6.2	156
42	Polycrystalline ZnO: B grown by LPCVD as TCO for thin film silicon solar cells. Thin Solid Films, 2010, 518, 2961-2966.	1.8	155
43	Hydrogen-doped indium oxide/indium tin oxide bilayers for high-efficiency silicon heterojunction solar cells. Solar Energy Materials and Solar Cells, 2013, 115, 151-156.	6.2	153
44	25.1%-Efficient Monolithic Perovskite/Silicon Tandem Solar Cell Based on a <i>p</i> -type Monocrystalline Textured Silicon Wafer and High-Temperature Passivating Contacts. ACS Energy Letters, 2019, 4, 844-845.	17.4	152
45	Photocatalytic degradation of phenol by TiO2 thin films prepared by sputtering. Applied Catalysis B: Environmental, 2000, 25, 83-92.	20.2	151
46	Amorphous Si Thin Film Based Photocathodes with High Photovoltage for Efficient Hydrogen Production. Nano Letters, 2013, 13, 5615-5618.	9.1	151
47	Optimization of amorphous silicon thin film solar cells for flexible photovoltaics. Journal of Applied Physics, 2008, 103, .	2.5	147
48	Integrated thinking for photovoltaics in buildings. Nature Energy, 2018, 3, 438-442.	39.5	146
49	Improving metal reflectors by suppressing surface plasmon polaritons: a priori calculation of the internal reflectance of a solar cell. Light: Science and Applications, 2013, 2, e106-e106.	16.6	143
50	New Crystal Structures of WS2: Microtubes, Ribbons, and Ropes. Advanced Materials, 1998, 10, 246-249.	21.0	140
51	Status and perspectives of crystalline silicon photovoltaics in research and industry. Nature Reviews Materials, 2022, 7, 597-616.	48.7	139
52	Comparison and optimization of randomly textured surfaces in thin-film solar cells. Optics Express, 2010, 18, A335.	3.4	138
53	Review: Progress in solar cells from hydrogenated amorphous silicon. Renewable and Sustainable Energy Reviews, 2017, 76, 1497-1523.	16.4	134
54	Modeling of light scattering from micro- and nanotextured surfaces. Journal of Applied Physics, 2010, 107, 044504.	2.5	132

#	Article	IF	CITATIONS
55	I <sub>2</sub> vapor-induced degradation of formamidinium lead iodide based perovskite solar cells under heat–light soaking conditions. Energy and Environmental Science, 2019, 12, 3074-3088.	30.8	131
56	Fracture strength and Young's modulus of ZnO nanowires. Nanotechnology, 2007, 18, 205503.	2.6	130
57	Multiscale Transparent Electrode Architecture for Efficient Light Management and Carrier Collection in Solar Cells. Nano Letters, 2012, 12, 1344-1348.	9.1	127
58	Stretched-exponential a-Si:Hâ^•c-Si interface recombination decay. Applied Physics Letters, 2008, 93, .	3.3	123
59	Organic–Inorganic Halide Perovskites: Perspectives for Silicon-Based Tandem Solar Cells. IEEE Journal of Photovoltaics, 2014, 4, 1545-1551.	2.5	123
60	Mixed-phase p-type silicon oxide containing silicon nanocrystals and its role in thin-film silicon solar cells. Applied Physics Letters, 2010, 97, .	3.3	119
61	Silicon Filaments in Silicon Oxide for Nextâ€Generation Photovoltaics. Advanced Materials, 2012, 24, 1182-1186.	21.0	118
62	Resistive interlayer for improved performance of thin film silicon solar cells on highly textured substrate. Applied Physics Letters, 2010, 96, .	3.3	116
63	In Situ TEM Analysis of Organic–Inorganic Metal-Halide Perovskite Solar Cells under Electrical Bias. Nano Letters, 2016, 16, 7013-7018.	9.1	115
64	Realization of GalnP/Si Dual-Junction Solar Cells With 29.8% 1-Sun Efficiency. IEEE Journal of Photovoltaics, 2016, 6, 1012-1019.	2.5	114
65	Amorphous silicon oxide window layers for high-efficiency silicon heterojunction solar cells. Journal of Applied Physics, 2014, 115, .	2.5	113
66	Low-Temperature High-Mobility Amorphous IZO for Silicon Heterojunction Solar Cells. IEEE Journal of Photovoltaics, 2015, 5, 1340-1347.	2.5	113
67	Photocurrent enhancement in thin film amorphous silicon solar cells with silver nanoparticles. Progress in Photovoltaics: Research and Applications, 2011, 19, 260-265.	8.1	111
68	Solar cell efficiency enhancement via light trapping in printable resonant dielectric nanosphere arrays. Physica Status Solidi (A) Applications and Materials Science, 2013, 210, 255-260.	1.8	109
69	Laser-Scribing Patterning for the Production of Organometallic Halide Perovskite Solar Modules. IEEE Journal of Photovoltaics, 2015, 5, 1087-1092.	2.5	109
70	A passivating contact for silicon solar cells formed during a single firing thermal annealing. Nature Energy, 2018, 3, 800-808.	39.5	109
71	Axial p-n Junctions Realized in Silicon Nanowires by Ion Implantation. Nano Letters, 2009, 9, 1341-1344.	9.1	107
72	Zinc tin oxide as high-temperature stable recombination layer for mesoscopic perovskite/silicon monolithic tandem solar cells. Applied Physics Letters, 2016, 109, .	3.3	105

#	Article	IF	CITATIONS
73	Deformation mechanisms of silicon during nanoscratching. Physica Status Solidi (A) Applications and Materials Science, 2005, 202, 2858-2869.	1.8	102
74	Optical management in high-efficiency thin-film silicon micromorph solar cells with a silicon oxide based intermediate reflector. Physica Status Solidi - Rapid Research Letters, 2008, 2, 163-165.	2.4	102
75	Silicon Heterojunction Solar Cells With Copper-Plated Grid Electrodes: Status and Comparison With Silver Thick-Film Techniques. IEEE Journal of Photovoltaics, 2014, 4, 1055-1062.	2.5	96
76	Simple processing of back-contacted silicon heterojunction solar cells using selective-area crystalline growth. Nature Energy, 2017, 2, .	39.5	95
77	Geometric light trapping for high efficiency thin film silicon solar cells. Solar Energy Materials and Solar Cells, 2012, 98, 185-190.	6.2	94
78	Record Infrared Internal Quantum Efficiency in Silicon Heterojunction Solar Cells With Dielectric/Metal Rear Reflectors. IEEE Journal of Photovoltaics, 2013, 3, 1243-1249.	2.5	92
79	Monolithic Perovskite‧ilicon Tandem Solar Cells: From the Lab to Fab?. Advanced Materials, 2022, 34, e2106540.	21.0	92
80	Amorphous/crystalline silicon interface defects induced by hydrogen plasma treatments. Applied Physics Letters, 2013, 102, .	3.3	91
81	Light management in thin film silicon solar cells. Energy and Environmental Science, 2015, 8, 824-837.	30.8	91
82	Development of micromorph tandem solar cells on flexible low-cost plastic substrates. Solar Energy Materials and Solar Cells, 2009, 93, 884-887.	6.2	90
83	Photocurrent increase in n-i-p thin film silicon solar cells by guided mode excitation via grating coupler. Applied Physics Letters, 2010, 96, .	3.3	90
84	The silane depletion fraction as an indicator for the amorphous/crystalline silicon interface passivation quality. Applied Physics Letters, 2010, 97, .	3.3	90
85	Highâ€efficiency microcrystalline silicon singleâ€junction solar cells. Progress in Photovoltaics: Research and Applications, 2013, 21, 821-826.	8.1	90
86	Passivating electron contact based on highly crystalline nanostructured silicon oxide layers for silicon solar cells. Solar Energy Materials and Solar Cells, 2016, 158, 2-10.	6.2	90
87	An Indiumâ€Free Anode for Largeâ€Area Flexible OLEDs: Defectâ€Free Transparent Conductive Zinc Tin Oxide. Advanced Functional Materials, 2016, 26, 384-392.	14.9	90
88	Structural, chemical, and electrical characterisation of reactively sputtered WSx thin films. Thin Solid Films, 1996, 280, 67-75.	1.8	89
89	Complex Refractive Indices of Cesium–Formamidinium-Based Mixed-Halide Perovskites with Optical Band Gaps from 1.5 to 1.8 eV. ACS Energy Letters, 2018, 3, 742-747.	17.4	89
90	Efficient nanocoaxâ€based solar cells. Physica Status Solidi - Rapid Research Letters, 2010, 4, 181-183.	2.4	87

#	Article	IF	CITATIONS
91	Perovskite/Perovskite/Silicon Monolithic Triple-Junction Solar Cells with a Fully Textured Design. ACS Energy Letters, 2018, 3, 2052-2058.	17.4	87
92	Solar glass with industrial porous SiO2 antireflection coating: measurements of photovoltaic module properties improvement and modelling of yearly energy yield gain. Solar Energy Materials and Solar Cells, 2004, 82, 331-344.	6.2	86
93	Solar-to-Hydrogen Production at 14.2% Efficiency with Silicon Photovoltaics and Earth-Abundant Electrocatalysts. Journal of the Electrochemical Society, 2016, 163, F1177-F1181.	2.9	85
94	Solar Water Splitting with Perovskite/Silicon Tandem Cell and TiC-Supported Pt Nanocluster Electrocatalyst. Joule, 2019, 3, 2930-2941.	24.0	85
95	Recent advances and remaining challenges in thin-film silicon photovoltaic technology. Materials Today, 2015, 18, 378-384.	14.2	83
96	Optimization of thin film silicon solar cells on highly textured substrates. Physica Status Solidi (A) Applications and Materials Science, 2011, 208, 1863-1868.	1.8	82
97	Nanocrystalline Silicon Carrier Collectors for Silicon Heterojunction Solar Cells and Impact on Low-Temperature Device Characteristics. IEEE Journal of Photovoltaics, 2016, 6, 1654-1662.	2.5	82
98	Growth Model of MOCVD Polycrystalline ZnO. Crystal Growth and Design, 2009, 9, 4957-4962.	3.0	81
99	Light Management: A Key Concept in High-Efficiency Perovskite/Silicon Tandem Photovoltaics. Journal of Physical Chemistry Letters, 2019, 10, 3159-3170.	4.6	81
100	Solar Hydrogen Production by Amorphous Silicon Photocathodes Coated with a Magnetron Sputter Deposited Mo <sub>2</sub> C Catalyst. Journal of the American Chemical Society, 2015, 137, 7035-7038.	13.7	80
101	Parasitic Absorption Reduction in Metal Oxide-Based Transparent Electrodes: Application in Perovskite Solar Cells. ACS Applied Materials & Interfaces, 2016, 8, 17260-17267.	8.0	80
102	Interplay of annealing temperature and doping in hole selective rear contacts based on silicon-rich silicon-carbide thin films. Solar Energy Materials and Solar Cells, 2017, 173, 18-24.	6.2	79
103	TCOs for nip thin film silicon solar cells. Progress in Photovoltaics: Research and Applications, 2009, 17, 165-176.	8.1	78
104	Low-Temperature Screen-Printed Metallization for the Scale-Up of Two-Terminal Perovskite–Silicon Tandems. ACS Applied Energy Materials, 2019, 2, 3815-3821.	5.1	78
105	The impact of silicon solar cell architecture and cell interconnection on energy yield in hot & sunny climates. Energy and Environmental Science, 2017, 10, 1196-1206.	30.8	76
106	Instability of p–i–n perovskite solar cells under reverse bias. Journal of Materials Chemistry A, 2020, 8, 242-250.	10.3	76
107	Asymmetric intermediate reflector for tandem micromorph thin film silicon solar cells. Applied Physics Letters, 2009, 94, .	3.3	75
108	Parasitic absorption in the rear reflector of a silicon solar cell: Simulation and measurement of the sub-bandgap reflectance for common dielectric/metal reflectors. Solar Energy Materials and Solar Cells, 2014, 120, 426-430.	6.2	75

#		IF	CITATIONS
109	Very fast light-induced degradation of <mml:math xmins:mml="http://www.w3.org/1998/Math/Math/MathML&lt;br">display="inline"&gt;<mml:mrow><mml:mi>a</mml:mi></mml:mrow></mml:math> -Si:H/ <mml:math xmlns:mml="http://www.w3.org/1998/Math/MathML" display="inline"&gt;<mml:mrow><mml:mi>c</mml:mi></mml:mrow>-Si(100) interfaces.</mml:math 	3.2	74
110	Hysical Review B, 2011, 85, . UVâ€nanoâ€imprint lithography technique for the replication of back reflectors for nâ€iâ€p thin film silicon solar cells. Progress in Photovoltaics: Research and Applications, 2011, 19, 202-210.	8.1	74
111	A New View of Microcrystalline Silicon: The Role of Plasma Processing in Achieving a Dense and Stable Absorber Material for Photovoltaic Applications. Advanced Functional Materials, 2012, 22, 3665-3671.	14.9	74
112	Hole-Collection Mechanism in Passivating Metal-Oxide Contacts on Si Solar Cells: Insights From Numerical Simulations. IEEE Journal of Photovoltaics, 2018, 8, 473-482.	2.5	71
113	Back-Contacted Silicon Heterojunction Solar Cells With Efficiency >21%. IEEE Journal of Photovoltaics, 2014, 4, 1046-1054.	2.5	70
114	Impact of metal silicide precipitate dissolution during rapid thermal processing of multicrystalline silicon solar cells. Applied Physics Letters, 2005, 87, 121918.	3.3	69
115	Window layer with p doped silicon oxide for high V <i>oc</i> thin-film silicon n-i-p solar cells. Journal of Applied Physics, 2011, 110, . Kinetics of <mml:math <="" td="" xmlns:mml="http://www.w3.org/1998/Math/MathML"><td>2.5</td><td>69</td></mml:math>	2.5	69
116	display="inline"> <mml:mi>a</mml:mi> -Si:H bulk defect and <mml:math xmlns:mml="http://www.w3.org/1998/Math/MathML" display="inline"&gt;<mml:mi>a</mml:mi>-Si:H/<mml:math xmlns:mml="http://www.w3.org/1998/Math/MathML"</mml:math </mml:math 	3.2	69
117	display="inline"> <mml:mi>c</mml:mi> -Si interface-state reduction. Physical Review B, 2012, Field Performance versus Standard Test Condition Efficiency of Tandem Solar Cells and the Singular Case of Perovskites/Silicon Devices. Journal of Physical Chemistry Letters, 2018, 9, 446-458.	4.6	69
118	Light-induced performance increase of silicon heterojunction solar cells. Applied Physics Letters, 2016, 109, .	3.3	67
119	Mechanisms of wafer sawing and impact on wafer properties. Progress in Photovoltaics: Research and Applications, 2010, 18, 563-572.	8.1	65
120	Optimized short-circuit current mismatch in multi-junction solar cells. Solar Energy Materials and Solar Cells, 2013, 117, 120-125.	6.2	65
121	Increasing the efficiency of silicon heterojunction solar cells and modules by light soaking. Solar Energy Materials and Solar Cells, 2017, 173, 43-49.	6.2	65
122	Optical and electrical properties of semiconducting WS2 thin films: From macroscopic to local probe measurements. Solar Energy Materials and Solar Cells, 1999, 57, 189-207.	6.2	64
123	Resonances and absorption enhancement in thin film silicon solar cells with periodic interface texture. Journal of Applied Physics, 2011, 109, 084516.	2.5	64
124	Properties of interfaces in amorphous/crystalline silicon heterojunctions. Physica Status Solidi (A) Applications and Materials Science, 2010, 207, 651-656.	1.8	63
125	Efficient light management scheme for thin film silicon solar cells via transparent random nanostructures fabricated by nanoimprinting. Applied Physics Letters, 2010, 96, .	3.3	63
126	Economic viability for residential battery storage systems in grid onnected PV plants. IET Renewable Power Generation, 2018, 12, 135-142.	3.1	61

#	Article	lF	CITATIONS
127	Temperature dependence of the conductivity in large-grained boron-doped ZnO films. Solar Energy Materials and Solar Cells, 2007, 91, 1269-1274.	6.2	60
128	Carrier transport and sensitivity issues in heterojunction with intrinsic thin layer solar cells on N-type crystalline silicon: A computer simulation study. Journal of Applied Physics, 2010, 107, 054521.	2.5	60
129	Relaxing the Conductivity/Transparency Tradeâ€Off in MOCVD ZnO Thin Films by Hydrogen Plasma. Advanced Functional Materials, 2013, 23, 5177-5182.	14.9	60
130	Amorphous silicon–germanium for triple and quadruple junction thin-film silicon based solar cells. Solar Energy Materials and Solar Cells, 2015, 133, 163-169.	6.2	60
131	High fidelity transfer of nanometric random textures by UV embossing for thin film solar cells applications. Solar Energy Materials and Solar Cells, 2011, 95, 881-886.	6.2	58
132	Silicon-Rich Silicon Carbide Hole-Selective Rear Contacts for Crystalline-Silicon-Based Solar Cells. ACS Applied Materials & Interfaces, 2016, 8, 35660-35667.	8.0	57
133	Microcrystalline silicon solar cells: effect of substrate temperature on cracks and their role in postâ€oxidation. Progress in Photovoltaics: Research and Applications, 2010, 18, 491-499.	8.1	56
134	High-Efficiency P-I-N Microcrystalline and Micromorph Thin Film Silicon Solar Cells Deposited on LPCVD Zno Coated Glass Substrates. , 2006, , .		55
135	Flexible micromorph tandem a-Si/μc-Si solar cells. Journal of Applied Physics, 2010, 107, 014507.	2.5	55
136	Thin-film silicon triple-junction solar cell with 12.5% stable efficiency on innovative flat light-scattering substrate. Journal of Applied Physics, 2012, 112, .	2.5	55
137	Mitigating Plasmonic Absorption Losses at Rear Electrodes in Highâ€Efficiency Silicon Solar Cells Using Dopantâ€Free Contact Stacks. Advanced Functional Materials, 2020, 30, 1907840.	14.9	55
138	Understanding of photocurrent enhancement in real thin film solar cells: towards optimal one-dimensional gratings. Optics Express, 2011, 19, 128.	3.4	54
139	Analysis of lateral transport through the inversion layer in amorphous silicon/crystalline silicon heterojunction solar cells. Journal of Applied Physics, 2013, 114, 074504.	2.5	54
140	Strategies for Doped Nanocrystalline Silicon Integration in Silicon Heterojunction Solar Cells. IEEE Journal of Photovoltaics, 2016, 6, 1132-1140.	2.5	54
141	High-Stable-Efficiency Tandem Thin-Film Silicon Solar Cell With Low-Refractive-Index Silicon-Oxide Interlayer. IEEE Journal of Photovoltaics, 2014, 4, 1368-1373.	2.5	52
142	ITO/MoOx/a-Si:H(i) Hole-Selective Contacts for Silicon Heterojunction Solar Cells: Degradation Mechanisms and Cell Integration. IEEE Journal of Photovoltaics, 2017, 7, 1584-1590.	2.5	52
143	Deep reinforcement learning control of electric vehicle charging in the presence of photovoltaic generation. Applied Energy, 2021, 301, 117504.	10.1	52
144	Stabilization of the rhombohedral polytype in MoS2 and WS2 microtubes: TEM and AFM study. Surface Science, 1999, 433-435, 637-641.	1.9	51

#	Article	IF	CITATIONS
145	Influence of the ZnO buffer on the guided mode structure in Si/ZnO/Ag multilayers. Journal of Applied Physics, 2009, 106, .	2.5	50
146	Control of CVD-deposited ZnO films properties through water/DEZ ratio: Decoupling of electrode morphology and electrical characteristics. Solar Energy Materials and Solar Cells, 2012, 105, 46-52.	6.2	50
147	Comparison of amorphous silicon absorber materials: Light-induced degradation and solar cell efficiency. Journal of Applied Physics, 2013, 114, 154509.	2.5	50
148	35Âyears of photovoltaics: Analysis of the TISOâ€10â€kW solar plant, lessons learnt in safety and performance—Part 1. Progress in Photovoltaics: Research and Applications, 2019, 27, 328-339.	8.1	49
149	Influence of the Subcell Properties on the Fill Factor of Two-Terminal Perovskite–Silicon Tandem Solar Cells. ACS Energy Letters, 2020, 5, 1077-1082.	17.4	49
150	Atomic-Layer-Deposited Transparent Electrodes for Silicon Heterojunction Solar Cells. IEEE Journal of Photovoltaics, 2014, 4, 1387-1396.	2.5	48
151	Control of LPCVD ZnO growth modes for improved light trapping in thin film silicon solar cells. Solar Energy Materials and Solar Cells, 2011, 95, 1031-1034.	6.2	47
152	Environmental stability of high-mobility indium-oxide based transparent electrodes. APL Materials, 2015, 3, 116105.	5.1	47
153	Highly transparent modulated surface textured front electrodes for highâ€efficiency multijunction thinâ€film silicon solar cells. Progress in Photovoltaics: Research and Applications, 2015, 23, 949-963.	8.1	46
154	Highly Conductive and Broadband Transparent Zr-Doped In <sub>2</sub> O <sub>3</sub> as Front Electrode for Solar Cells. IEEE Journal of Photovoltaics, 2018, 8, 1202-1207.	2.5	46
155	Back-Contacted Silicon Heterojunction Solar Cells: Optical-Loss Analysis and Mitigation. IEEE Journal of Photovoltaics, 2015, 5, 1293-1303.	2.5	45
156	Charge Collection in Hybrid Perovskite Solar Cells: Relation to the Nanoscale Elemental Distribution. IEEE Journal of Photovoltaics, 2017, 7, 590-597.	2.5	45
157	Cleavage Fracture of Brittle Semiconductors from the Nanometre to the Centimetre Scale. Advanced Engineering Materials, 2005, 7, 309-317.	3.5	44
158	Manufacturing 100-µm-thick silicon solar cells with efficiencies greater than 20% in a pilot production line. Physica Status Solidi (A) Applications and Materials Science, 2015, 212, 13-24.	1.8	44
159	Design of perovskite/crystalline-silicon monolithic tandem solar cells. Optics Express, 2018, 26, A579.	3.4	44
160	Phosphorous-Doped Silicon Carbide as Front-Side Full-Area Passivating Contact for Double-Side Contacted c-Si Solar Cells. IEEE Journal of Photovoltaics, 2019, 9, 346-354.	2.5	44
161	Preparation and Photoelectrochemistry of Semiconducting WS2Thin Films. Journal of Physical Chemistry B, 1997, 101, 2485-2490.	2.6	43
162	Determination of Raman emission cross-section ratio in hydrogenated microcrystalline silicon. Journal of Non-Crystalline Solids, 2006, 352, 1200-1203.	3.1	43

#	Article	IF	CITATIONS
163	Micromorph thin-film silicon solar cells with transparent high-mobility hydrogenated indium oxide front electrodes. Journal of Applied Physics, 2011, 109, .	2.5	43
164	Silicon oxide buffer layer at the p–i interface in amorphous and microcrystalline silicon solar cells. Solar Energy Materials and Solar Cells, 2014, 120, 143-150.	6.2	43
165	Infrared laser-based monitoring of the silane dissociation during deposition of silicon thin films. Applied Physics Letters, 2009, 94, .	3.3	42
166	Highly reflective nanotextured sputtered silver back reflector for flexible high-efficiency n–i–p thin-film silicon solar cells. Solar Energy Materials and Solar Cells, 2011, 95, 3585-3591.	6.2	42
167	Optimization of ZnO Front Electrodes for High-Efficiency Micromorph Thin-Film Si Solar Cells. IEEE Journal of Photovoltaics, 2012, 2, 229-235.	2.5	42
168	Toward Annealingâ€Stable Molybdenumâ€Oxideâ€Based Holeâ€Selective Contacts For Silicon Photovoltaics. Solar Rrl, 2018, 2, 1700227.	5.8	42
169	Recombination Analysis of Phosphorus-Doped Nanostructured Silicon Oxide Passivating Electron Contacts for Silicon Solar Cells. IEEE Journal of Photovoltaics, 2018, 8, 389-396.	2.5	42
170	Low-temperature processes for passivation and metallization of high-efficiency crystalline silicon solar cells. Solar Energy, 2018, 175, 54-59.	6.1	42
171	Toward Stable Monolithic Perovskite/Silicon Tandem Photovoltaics: A Six-Month Outdoor Performance Study in a Hot and Humid Climate. ACS Energy Letters, 2021, 6, 2944-2951.	17.4	42
172	Cross-sectional electrostatic force microscopy of thin-film solar cells. Journal of Applied Physics, 2001, 89, 1418-1424.	2.5	41
173	Spectrally Selective Mid-Wave Infrared Detection Using Fabry-Pérot Cavity Enhanced Black Phosphorus 2D Photodiodes. ACS Nano, 2020, 14, 13645-13651.	14.6	41
174	Extended light scattering model incorporating coherence for thin-film silicon solar cells. Journal of Applied Physics, 2011, 110, .	2.5	40
175	Origin of the Voc enhancement with a p-doped nc-SiOx:H window layer in n-i-p solar cells. Journal of Non-Crystalline Solids, 2012, 358, 1958-1961.	3.1	40
176	Crystalline Silicon Solar Cells With Coannealed Electron- and Hole-Selective SiC <i> <sub>x</sub> </i> Passivating Contacts. IEEE Journal of Photovoltaics, 2018, 8, 1478-1485.	2.5	39
177	Highly transparent ZnO bilayers by LP-MOCVD as front electrodes for thin-film micromorph silicon solar cells. Solar Energy Materials and Solar Cells, 2012, 98, 331-336.	6.2	38
178	Experimental study of flat light-scattering substrates in thin-film silicon solar cells. Solar Energy Materials and Solar Cells, 2012, 101, 193-199.	6.2	38
179	Compressiveâ€shear adhesion characterization of polyvinylâ€butyral and ethyleneâ€vinyl acetate at different curing times before and after exposure to dampâ€heat conditions. Progress in Photovoltaics: Research and Applications, 2014, 22, 405-414.	8.1	38
180	Transparent Electrodes in Silicon Heterojunction Solar Cells: Influence on Contact Passivation. IEEE Journal of Photovoltaics, 2016, 6, 17-27.	2.5	38

#	Article	IF	CITATIONS
181	Analysis of hydrogen distribution and migration in fired passivating contacts (FPC). Solar Energy Materials and Solar Cells, 2019, 200, 110018.	6.2	38
182	Annealing of Silicon Heterojunction Solar Cells: Interplay of Solar Cell and Indium Tin Oxide Properties. IEEE Journal of Photovoltaics, 2019, 9, 1202-1207.	2.5	37
183	Vapor deposition of metal halide perovskite thin films: Process control strategies to shape layer properties. APL Materials, 2021, 9, .	5.1	37
184	Improvement of the open circuit voltage by modifying the transparent indium–tin oxide front electrode in amorphous n–i–p solar cells. Progress in Photovoltaics: Research and Applications, 2012, 20, 727-734.	8.1	36
185	Microcrystalline silicon deposited at high rate on large areas from pure silane with efficient gas utilization. Solar Energy Materials and Solar Cells, 2007, 91, 495-502.	6.2	35
186	Electrical transport in boronâ€doped polycrystalline zinc oxide thin films. Physica Status Solidi (A) Applications and Materials Science, 2008, 205, 1983-1987.	1.8	35
187	Laser applications in thin-film photovoltaics. Applied Physics B: Lasers and Optics, 2010, 100, 427-436.	2.2	35
188	c-texture versus a-texture low pressure metalorganic chemical vapor deposition ZnO films: Lower resistivity despite smaller grain size. Thin Solid Films, 2014, 565, 1-6.	1.8	35
189	<italic>In-Situ</italic> Monitoring of Moisture Ingress in PV Modules Using Digital Humidity Sensors. IEEE Journal of Photovoltaics, 2016, 6, 1152-1159.	2.5	35
190	Preparation and characterization of highly oriented, photoconducting WS2 thin films. Applied Physics A: Materials Science and Processing, 1996, 62, 543-546.	2.3	34
191	Humid environment stability of low pressure chemical vapor deposited boron doped zinc oxide used as transparent electrodes in thin film silicon solar cells. Thin Solid Films, 2011, 520, 558-562.	1.8	34
192	The development of high performance SnO2:F as TCOs for thin film silicon solar cells. Surface and Coatings Technology, 2012, 213, 167-174.	4.8	34
193	Technological status of plasma-deposited thin-film silicon photovoltaics. Solar Energy Materials and Solar Cells, 2013, 119, 311-316.	6.2	34
194	Control algorithm for a residential photovoltaic system with storage. Applied Energy, 2017, 202, 78-87.	10.1	34
195	Class AAA LED-Based Solar Simulator for Steady-State Measurements and Light Soaking. IEEE Journal of Photovoltaics, 2014, 4, 1282-1287.	2.5	33
196	35 years of photovoltaics: Analysis of the TISOâ€10â€kW solar plant, lessons learnt in safety and performance—Part 2. Progress in Photovoltaics: Research and Applications, 2019, 27, 760-778.	8.1	33
197	Low-Temperature \$p\$-Type Microcrystalline Silicon as Carrier Selective Contact for Silicon Heterojunction Solar Cells. IEEE Journal of Photovoltaics, 2019, 9, 1158-1165.	2.5	33
198	Influence of Light Soaking on Silicon Heterojunction Solar Cells With Various Architectures. IEEE Journal of Photovoltaics, 2021, 11, 575-583.	2.5	33

#	Article	IF	CITATIONS
199	Optical transmission as a fast and nonâ€destructive tool for determination of ethyleneâ€coâ€vinyl acetate curing state in photovoltaic modules. Progress in Photovoltaics: Research and Applications, 2013, 21, 187-194.	8.1	32
200	Plastic and Elastic Strain Fields in GaAs/Si Core–Shell Nanowires. Nano Letters, 2014, 14, 1859-1864.	9.1	32
201	Amorphous/Crystalline Silicon Interface Passivation: Ambient-Temperature Dependence and Implications for Solar Cell Performance. IEEE Journal of Photovoltaics, 2015, 5, 718-724.	2.5	32
202	Wire-sawing processes: parametrical study and modeling. Solar Energy Materials and Solar Cells, 2015, 132, 392-402.	6.2	32
203	Closing the Cell-to-Module Efficiency Gap: A Fully Laser Scribed Perovskite Minimodule With 16% Steady-State Aperture Area Efficiency. IEEE Journal of Photovoltaics, 2018, 8, 151-155.	2.5	32
204	Lateral transport in silicon solar cells. Journal of Applied Physics, 2020, 127, .	2.5	32
205	Dicing of gallium–arsenide high performance laser diodes for industrial applications. Journal of Materials Processing Technology, 2008, 198, 114-121.	6.3	31
206	Substrate dependent stability and interplay between optical and electrical properties in μc-Si:H single junction solar cells. Solar Energy Materials and Solar Cells, 2011, 95, 195-198.	6.2	31
207	Light trapping in solar cells: Analytical modeling. Applied Physics Letters, 2012, 101, .	3.3	31
208	Enhancing the optoelectronic properties of amorphous zinc tin oxide by subgap defect passivation: A theoretical and experimental demonstration. Physical Review B, 2017, 95, .	3.2	31
209	Nano-emitting Heterostructures Violate Optical Reciprocity and Enable Efficient Photoluminescence in Halide-Segregated Methylammonium-Free Wide Bandgap Perovskites. ACS Energy Letters, 2021, 6, 419-428.	17.4	31
210	Crystallinity and texture promotion in WS2 thin films. Journal of Vacuum Science and Technology A: Vacuum, Surfaces and Films, 1997, 15, 2323-2329.	2.1	30
211	Radiation hardness of amorphous silicon particle sensors. Journal of Non-Crystalline Solids, 2006, 352, 1797-1800.	3.1	30
212	Light trapping in solar cells: When does a Lambertian scatterer scatter Lambertianly?. Journal of Applied Physics, 2012, 112, .	2.5	30
213	Plasmonic silicon solar cells: impact of material quality and geometry. Optics Express, 2013, 21, A786.	3.4	30
214	Hydrogen plasma treatment for improved conductivity in amorphous aluminum doped zinc tin oxide thin films. APL Materials, 2014, 2, 096113.	5.1	30
215	Thin-Film Silicon Triple-Junction Solar Cells on Highly Transparent Front Electrodes With Stabilized Efficiencies up to 12.8%. IEEE Journal of Photovoltaics, 2014, 4, 757-762.	2.5	30
216	Silicon Heterojunction Solar Cells: Towards Low-cost High-Efficiency Industrial Devices and Application to Low-concentration PV. Energy Procedia, 2015, 77, 508-514.	1.8	30

#	Article	IF	CITATIONS
217	Metallization of Si heterojunction solar cells by nanosecond laser ablation and Ni-Cu plating. Solar Energy Materials and Solar Cells, 2017, 159, 243-250.	6.2	30
218	N/I buffer layer for substrate microcrystalline thin film silicon solar cell. Journal of Applied Physics, 2008, 104, 104505.	2.5	29
219	Influence of pressure and silane depletion on microcrystalline silicon material quality and solar cell performance. Journal of Applied Physics, 2009, 105, 064507.	2.5	29
220	On the Interplay Between Microstructure and Interfaces in High-Efficiency Microcrystalline Silicon Solar Cells. IEEE Journal of Photovoltaics, 2013, 3, 11-16.	2.5	29
221	New progress in the fabrication of n–i–p micromorph solar cells for opaque substrates. Solar Energy Materials and Solar Cells, 2013, 114, 147-155.	6.2	29
222	Light and durable: <scp>C</scp> omposite structures for buildingâ€integrated photovoltaic modules. Progress in Photovoltaics: Research and Applications, 2018, 26, 718-729.	8.1	29
223	Aluminium-Doped Zinc Oxide Rear Reflectors for High-Efficiency Silicon Heterojunction Solar Cells. IEEE Journal of Photovoltaics, 2019, 9, 1217-1224.	2.5	29
224	Characterisation of rough reflecting substrates incorporated into thin-film silicon solar cells. Progress in Photovoltaics: Research and Applications, 2006, 14, 485-498.	8.1	28
225	Unlinking absorption and haze in thin film silicon solar cells front electrodes. Physica Status Solidi - Rapid Research Letters, 2010, 4, 326-328.	2.4	28
226	Copper and Transparent-Conductor Reflectarray Elements on Thin-Film Solar Cell Panels. IEEE Transactions on Antennas and Propagation, 2014, 62, 3813-3818.	5.1	28
227	A Physically-Based Electrical Model for Lithium-Ion Cells. IEEE Transactions on Energy Conversion, 2019, 34, 594-603.	5.2	28
228	Temperature dependence of hydrogenated amorphous silicon solar cell performances. Journal of Applied Physics, 2016, 119, .	2.5	27
229	Numerical simulations of hole carrier selective contacts in p-type c-Si solar cells. Solar Energy Materials and Solar Cells, 2019, 200, 109937.	6.2	27
230	Dopantâ€Free Backâ€Contacted Silicon Solar Cells with an Efficiency of 22.1%. Physica Status Solidi - Rapid Research Letters, 2020, 14, 1900688.	2.4	27
231	Amorphous Silicon/Crystalline Silicon Heterojunction Solar Cells. Semiconductors and Semimetals, 2014, , 73-120.	0.7	26
232	Optimization of tunnel-junction IBC solar cells based on a series resistance model. Solar Energy Materials and Solar Cells, 2019, 200, 110036.	6.2	26
233	Robust Glass-Free Lightweight Photovoltaic Modules With Improved Resistance to Mechanical Loads and Impact. IEEE Journal of Photovoltaics, 2019, 9, 245-251.	2.5	26
234	Dicing of gallium–arsenide high performance laser diodes for industrial applications. Journal of Materials Processing Technology, 2008, 198, 105-113.	6.3	25

#	Article	IF	CITATIONS
235	Nanometer- and Micrometer-Scale Texturing for High-Efficiency Micromorph Thin-Film Silicon Solar Cells. IEEE Journal of Photovoltaics, 2012, 2, 83-87.	2.5	25
236	Light-induced Voc increase and decrease in high-efficiency amorphous silicon solar cells. Journal of Applied Physics, 2014, 116, 094503.	2.5	25
237	Exceedingly Cheap Perovskite Solar Cells Using Iron Pyrite Hole Transport Materials. ChemistrySelect, 2016, 1, 5316-5319.	1.5	25
238	Unsupervised algorithm for disaggregating low-sampling-rate electricity consumption of households. Sustainable Energy, Grids and Networks, 2019, 19, 100244.	3.9	25
239	Multimodal Microscale Imaging of Textured Perovskite–Silicon Tandem Solar Cells. ACS Energy Letters, 2021, 6, 2293-2304.	17.4	25
240	Realization of high efficiency micromorph tandem silicon solar cells on glass and plastic substrates: Issues and potential. Solar Energy Materials and Solar Cells, 2011, 95, 127-130.	6.2	24
241	Is light-induced degradation of <i>a-</i> Si:H/ <i>c</i> -Si interfaces reversible?. Applied Physics Letters, 2014, 104, .	3.3	24
242	When PV modules are becoming real building elements: White solar module, a revolution for BIPV. , 2015, , .		24
243	Rear-emitter silicon heterojunction solar cells with atomic layer deposited ZnO:Al serving as an alternative transparent conducting oxide to In2O3:Sn. Solar Energy Materials and Solar Cells, 2019, 200, 109953.	6.2	24
244	Alternative procedure for the fabrication of close-spaced sublimated CdTe solar cells. Journal of Vacuum Science and Technology A: Vacuum, Surfaces and Films, 2000, 18, 1599-1603.	2.1	23
245	Modification of textured silicon wafer surface morphology for fabrication of heterojunction solar cell with open circuit voltage over 700 mV. , 2009, , .		23
246	Effect of debris on the silicon wafering for solar cells. Solar Energy Materials and Solar Cells, 2011, 95, 2490-2496.	6.2	23
247	Analysis of onset of dislocation nucleation during nanoindentation and nanoscratching of InP. Journal of Materials Research, 2012, 27, 320-329.	2.6	23
248	Oneâ€ŧypeâ€fitsâ€allâ€systems: Strategies for preventing potentialâ€induced degradation in crystalline silicon solar photovoltaic modules. Progress in Photovoltaics: Research and Applications, 2019, 27, 13-21.	8.1	23
249	Exploring co-sputtering of ZnO:Al and SiO2 for efficient electron-selective contacts on silicon solar cells. Solar Energy Materials and Solar Cells, 2019, 194, 67-73.	6.2	23
250	The versatility of passivating carrierâ€selective silicon thin films for diverse highâ€efficiency screenâ€printed heterojunctionâ€based solar cells. Progress in Photovoltaics: Research and Applications, 2020, 28, 569-577.	8.1	23
251	Zr-doped indium oxide electrodes: Annealing and thickness effects on microstructure and carrier transport. Physical Review Materials, 2019, 3, .	2.4	23
252	Light absorption in textured thin film silicon solar cells: A simple scalar scattering approach versus rigorous simulation. Applied Physics Letters, 2011, 98, .	3.3	22

#	Article	IF	CITATIONS
253	Probing Photocurrent Nonuniformities in the Subcells of Monolithic Perovskite/Silicon Tandem Solar Cells. Journal of Physical Chemistry Letters, 2016, 7, 5114-5120.	4.6	22
254	Vapor Transport Deposition of Methylammonium Iodide for Perovskite Solar Cells. ACS Applied Energy Materials, 2021, 4, 4333-4343.	5.1	22
255	Low-temperature plasma-deposited silicon epitaxial films: Growth and properties. Journal of Applied Physics, 2014, 116, .	2.5	21
256	From randomly self-textured substrates to highly efficient thin film solar cells: Influence of geometric interface engineering on light trapping, plasmonic losses and charge extraction. Solar Energy Materials and Solar Cells, 2017, 160, 141-148.	6.2	21
257	Thermo-mechanical stability of lightweight glass-free photovoltaic modules based on a composite substrate. Solar Energy Materials and Solar Cells, 2018, 187, 82-90.	6.2	21
258	Rule-based scheduling of air conditioning using occupancy forecasting. Energy and Al, 2020, 2, 100022.	10.6	21
259	Effects of X-rays on Perovskite Solar Cells. Journal of Physical Chemistry C, 2020, 124, 17949-17956.	3.1	21
260	LPCVD ZnO-based intermediate reflector for micromorph tandem solar cells. Solar Energy Materials and Solar Cells, 2011, 95, 2161-2166.	6.2	20
261	High-efficiency Silicon Heterojunction Solar Cells: A Review. Green, 2012, .	0.4	20
262	Compositional study of defects in microcrystalline silicon solar cells using spectral decomposition in the scanning transmission electron microscope. Applied Physics Letters, 2013, 102, .	3.3	20
263	Review of amorphous silicon based particle detectors: the quest for single particle detection. Semiconductor Science and Technology, 2016, 31, 103005.	2.0	20
264	22% efficient dopant-free interdigitated back contact silicon solar cells. AIP Conference Proceedings, 2018, , .	0.4	20
265	Micromorph Solar Cell Optimization using a ZnO Layer as Intermediate Reflector. , 2006, , .		19
266	Mixed phase silicon oxide layers for thin-film silicon solar cells. Materials Research Society Symposia Proceedings, 2011, 1321, 349.	0.1	19
267	UV imprinting for thin film solar cell application. Journal of Optics (United Kingdom), 2012, 14, 024009.	2.2	19
268	Light trapping in solar cells at the extreme coupling limit. Journal of the Optical Society of America B: Optical Physics, 2013, 30, 13.	2.1	19
269	9.4% Efficient Amorphous Silicon Solar Cell on High Aspectâ€Ratio Glass Microcones. Advanced Materials, 2014, 26, 4082-4086.	21.0	19
270	Increasing Polycrystalline Zinc Oxide Grain Size by Control of Film Preferential Orientation. Crystal Growth and Design, 2015, 15, 5886-5891.	3.0	19

#	Article	IF	CITATIONS
271	The Role of Water in the Reversible Optoelectronic Degradation of Hybrid Perovskites at Low Pressure. Journal of Physical Chemistry C, 2017, 121, 25659-25665.	3.1	19
272	Properties of mixed phase silicon-oxide-based passivating contacts for silicon solar cells. Solar Energy Materials and Solar Cells, 2018, 181, 9-14.	6.2	19
273	Cross-sectional atomic force microscopy imaging of polycrystalline thin films. Ultramicroscopy, 2000, 85, 61-71.	1.9	18
274	Limiting factors in the fabrication of microcrystalline silicon solar cells and microcrystalline/amorphous (â€~micromorph') tandems. Philosophical Magazine, 2009, 89, 2599-2621.	1.6	18
275	2-D Periodic and Random-on-Periodic Front Textures for Tandem Thin-Film Silicon Solar Cells. IEEE Journal of Photovoltaics, 2014, 4, 1177-1184.	2.5	18
276	Silver versus white sheet as a back reflector for microcrystalline silicon solar cells deposited on LPCVDâ€ZnO electrodes of various textures. Progress in Photovoltaics: Research and Applications, 2015, 23, 1182-1189.	8.1	18
277	Photocurrent Spectroscopy of Perovskite Layers and Solar Cells: A Sensitive Probe of Material Degradation. Journal of Physical Chemistry Letters, 2017, 8, 838-843.	4.6	18
278	Degradation Mechanism and Stability Improvement of Dopant-Free ZnO/LiF <i><sub>x</sub></i> /Al Electron Nanocontacts in Silicon Heterojunction Solar Cells. ACS Applied Nano Materials, 2020, 3, 11391-11398.	5.0	18
279	Design Rules to Fully Benefit From Bifaciality in Two-Terminal Perovskite/Silicon Tandem Solar Cells. IEEE Journal of Photovoltaics, 2020, 10, 714-721.	2.5	18
280	Preparation and characterization of highly oriented, photoconducting WS 2 thin films. Applied Physics A: Materials Science and Processing, 1996, 62, 543-546.	2.3	18
281	Diffraction and absorption enhancement from textured back reflectors of thin film solar cells. Journal of Applied Physics, 2012, 112, .	2.5	17
282	Time evolution of surface defect states in hydrogenated amorphous silicon studied by photothermal and photocurrent spectroscopy and optical simulation. Journal of Non-Crystalline Solids, 2012, 358, 2035-2038.	3.1	17
283	Self-Patterned Nanoparticle Layers for Vertical Interconnects: Application in Tandem Solar Cells. Nano Letters, 2014, 14, 5085-5091.	9.1	17
284	Fabrication and characterization of monolithically integrated microchannel plates based on amorphous silicon. Scientific Reports, 2014, 4, 4597.	3.3	17
285	Asymmetric band offsets in silicon heterojunction solar cells: Impact on device performance. Journal of Applied Physics, 2016, 120, 054501.	2.5	17
286	Progression towards high efficiency perovskite solar cells via optimisation of the front electrode and blocking layer. Journal of Materials Chemistry C, 2016, 4, 11269-11277.	5.5	17
287	Demonstrating the high Voc potential of PEDOT:PSS/c-Si heterojunctions on solar cells. Energy Procedia, 2017, 124, 593-597.	1.8	17
288	Industrialization of hybrid Si/III–V and translucent planar microâ€ŧracking modules. Progress in Photovoltaics: Research and Applications, 2021, 29, 819-834.	8.1	17

#	Article	IF	CITATIONS
289	Light-induced degradation of thin film amorphous and microcrystalline silicon solar cells. , 2005, , .		16
290	Tuning the porosity of zinc oxide electrodes: from dense to nanopillar films. Materials Research Express, 2015, 2, 075006.	1.6	16
291	Tuning the Optoelectronic Properties of ZnO:Al by Addition of Silica for Light Trapping in Highâ€Efficiency Crystalline Si Solar Cells. Advanced Materials Interfaces, 2016, 3, 1500462.	3.7	16
292	Reduction of the phosphorous cross-contamination in n–i–p solar cells prepared in a single-chamber PECVD reactor. Solar Energy Materials and Solar Cells, 2011, 95, 606-610.	6.2	15
293	Latest Developments of High-Efficiency Micromorph Tandem Silicon Solar Cells Implementing Innovative Substrate Materials and Improved Cell Design. IEEE Journal of Photovoltaics, 2012, 2, 236-240.	2.5	15
294	Variable light biasing method to measure component l–V characteristics of multi-junction solar cells. Solar Energy Materials and Solar Cells, 2012, 103, 128-133.	6.2	15
295	Hybrid axial and radial Si–GaAs heterostructures in nanowires. Nanoscale, 2013, 5, 9633.	5.6	15
296	Comparison of amorphous silicon absorber materials: Kinetics of lightâ€induced degradation. Progress in Photovoltaics: Research and Applications, 2016, 24, 446-457.	8.1	15
297	Spectrally resolved nonlinearity and temperature dependence of perovskite solar cells. Solar Energy Materials and Solar Cells, 2017, 172, 66-73.	6.2	15
298	Interdigitated back contact silicon heterojunction solar cells featuring an interband tunnel junction enabling simplified processing. Solar Energy, 2018, 175, 60-67.	6.1	15
299	New Route for "Cold-Passivation―of Defects in Tin-Based Oxides. Journal of Physical Chemistry C, 2018, 122, 17612-17620.	3.1	15
300	Field test and electrode optimization of electrodynamic cleaning systems for solar panels. Progress in Photovoltaics: Research and Applications, 2019, 27, 1020-1033.	8.1	15
301	Quantifying and modeling the impact of interconnection failures on the electrical performance of crystalline silicon photovoltaic modules. Progress in Photovoltaics: Research and Applications, 2019, 27, 424-432.	8.1	15
302	Vertical integration of hydrogenated amorphous silicon devices on CMOS circuits. Materials Research Society Symposia Proceedings, 2005, 869, 111.	0.1	14
303	Internal electric field and fill factor of amorphous silicon solar cells. , 2010, , .		14
304	Stencil-Nanopatterned Back Reflectors for Thin-Film Amorphous Silicon n-i-p Solar Cells. IEEE Journal of Photovoltaics, 2013, 3, 22-26.	2.5	14
305	The effect of cooling press on the encapsulation properties of crystalline photovoltaic modules: residual stress and adhesion. Progress in Photovoltaics: Research and Applications, 2015, 23, 160-169.	8.1	14
306	Profilometry of thin films on rough substrates by Raman spectroscopy. Scientific Reports, 2016, 6, 37859.	3.3	14

#	Article	IF	CITATIONS
307	Imaging the Spatial Evolution of Degradation in Perovskite/Si Tandem Solar Cells After Exposure to Humid Air. IEEE Journal of Photovoltaics, 2017, 7, 1563-1568.	2.5	14
308	Implementation and understanding of p+ fired rear hole selective tunnel oxide passivating contacts enabling >22% conversion efficiency in p-type c-Si solar cells. Solar Energy Materials and Solar Cells, 2021, 219, 110809.	6.2	14
309	Selective etching of n-InP(100) triggered at surface dislocations induced by nanoscratching. Electrochimica Acta, 2006, 51, 2182-2187.	5.2	13
310	ZnO transparent conductive oxide for thin film silicon solar cells. Proceedings of SPIE, 2010, , .	0.8	13
311	Excitation of guided-mode resonances in thin film silicon solar cells. Materials Research Society Symposia Proceedings, 2011, 1321, 123.	0.1	13
312	Angular behavior of the absorption limit in thin film silicon solar cells. Progress in Photovoltaics: Research and Applications, 2014, 22, 1147-1158.	8.1	13
313	Effect of the thin-film limit on the measurable optical properties of graphene. Scientific Reports, 2015, 5, 15684.	3.3	13
314	Amorphous gallium oxide grown by low-temperature PECVD. Journal of Vacuum Science and Technology A: Vacuum, Surfaces and Films, 2018, 36, 021518.	2.1	13
315	Record-Efficiency n-Type and High-Efficiency p-Type Monolike Silicon Heterojunction Solar Cells with a High-Temperature Gettering Process. ACS Applied Energy Materials, 2019, 2, 4900-4906.	5.1	13
316	Mitigating the impact of distributed PV in a low-voltage grid using electricity tariffs. Electric Power Systems Research, 2020, 189, 106763.	3.6	13
317	Kinetics of creation and of thermal annealing of light-induced defects in microcrystalline silicon solar cells. Journal of Applied Physics, 2008, 103, .	2.5	12
318	Electrothermal Finite-Element Modeling for Defect Characterization in Thin-Film Silicon Solar Modules. IEEE Journal of Selected Topics in Quantum Electronics, 2013, 19, 1-8.	2.9	12
319	Attenuated total reflectance Fourier-transform infrared spectroscopic investigation of silicon heterojunction solar cells. Review of Scientific Instruments, 2015, 86, 073108.	1.3	12
320	Survey of dopant-free carrier-selective contacts for silicon solar cells. , 2016, , .		12
321	1 cm2 CH3NH3PbI3 mesoporous solar cells with 17.8% steady-state efficiency by tailoring front FTO electrodes. Journal of Materials Chemistry C, 2017, 5, 4946-4950.	5.5	12
322	Zinc blende–wurtzite polytypism in nanocrystalline ZnO films. Acta Materialia, 2017, 130, 240-248.	7.9	12
323	Application-independent protocol for predicting the efficiency of lithium-ion battery cells in operations. Journal of Energy Storage, 2018, 15, 415-422.	8.1	12
324	Optimised Heat Pump Management for Increasing Photovoltaic Penetration into the Electricity Grid. Energies, 2019, 12, 1571.	3.1	12

#	Article	IF	CITATIONS
325	New Crystal Structures of WS2: Microtubes, Ribbons, and Ropes. Advanced Materials, 1998, 10, 246-249.	21.0	12
326	Submicron contacts for electrical characterization of semiconducting WS2 thin films. Journal of Vacuum Science and Technology A: Vacuum, Surfaces and Films, 1998, 16, 1239-1243.	2.1	11
327	The Nature and Origin of Lateral Composition Modulations in Short-Period Strained-Layer Superlattices. Materials Research Society Symposia Proceedings, 1999, 583, 297.	0.1	11
328	New Generation Transparent LPCVD ZnO Electrodes for Enhanced Photocurrent in Micromorph Solar Cells and Modules. IEEE Journal of Photovoltaics, 2012, 2, 88-93.	2.5	11
329	High-performance tandem silicon solar cells on F:SnO2. Surface and Coatings Technology, 2013, 230, 228-233.	4.8	11
330	Smoothening intermediate reflecting layer for tandem thin-film silicon solar cells. Solar Energy Materials and Solar Cells, 2013, 119, 12-17.	6.2	11
331	Thin-film silicon solar cells applying optically decoupled back reflectors. Materials Science and Engineering B: Solid-State Materials for Advanced Technology, 2013, 178, 645-650.	3.5	11
332	Limit of light coupling strength in solar cells. Applied Physics Letters, 2013, 102, 131113.	3.3	11
333	Tailoring the surface morphology of zinc oxide films for high-performance micromorph solar cells. Solar Energy Materials and Solar Cells, 2014, 128, 378-385.	6.2	11
334	Three-dimensional amorphous silicon solar cells on periodically ordered ZnO nanocolumns. Physica Status Solidi (A) Applications and Materials Science, 2015, 212, 1823-1829.	1.8	11
335	Microcrystalline silicon solar cells with passivated interfaces for high openâ€circuit voltage. Physica Status Solidi (A) Applications and Materials Science, 2015, 212, 840-845.	1.8	11
336	Comparison of LPCVD and sputter-etched ZnO layers applied as front electrodes in tandem thin-film silicon solar cells. Solar Energy Materials and Solar Cells, 2016, 145, 185-192.	6.2	11
337	Fourier light scattering model for treating textures deeper than the wavelength. Optics Express, 2017, 25, A14.	3.4	11
338	A Mixed-Phase SiO <sub>x</sub> Hole Selective Junction Compatible With High Temperatures Used in Industrial Solar Cell Manufacturing. IEEE Journal of Photovoltaics, 2020, 10, 1262-1269.	2.5	11
339	Hole-Selective Front Contact Stack Enabling 24.1%-Efficient Silicon Heterojunction Solar Cells. IEEE Journal of Photovoltaics, 2021, 11, 9-15.	2.5	11
340	Dopantâ€Free Bifacial Silicon Solar Cells. Solar Rrl, 2021, 5, 2000771.	5.8	11
341	Light trapping in thin-film solar cells measured by Raman spectroscopy. Applied Physics Letters, 2014, 105, 111106.	3.3	10
342	Practical silicon deposition rules derived from silane monitoring during plasma-enhanced chemical vapor deposition. Journal of Applied Physics, 2015, 117, .	2.5	10

#	Article	IF	CITATIONS
343	Accurate Determination of Photovoltaic Cell and Module Peak Power From Their Current–Voltage Characteristics. IEEE Journal of Photovoltaics, 2016, 6, 1564-1575.	2.5	10
344	Mechanical integrity of hybrid indium-free electrodes for flexible devices. Organic Electronics, 2016, 35, 136-141.	2.6	10
345	In-situ Determination of Moisture Diffusion Properties of PV Module Encapsulants Using Digital Humidity Sensors. , 2018, , .		10
346	Silicon oxide treatment to promote crystallinity of p-type microcrystalline layers for silicon heterojunction solar cells. AIP Conference Proceedings, 2018, , .	0.4	10
347	Optimization of front SiNx/ITO stacks for high-efficiency two-side contacted c-Si solar cells with co-annealed front and rear passivating contacts. Solar Energy Materials and Solar Cells, 2021, 219, 110815.	6.2	10
348	Palliating the efficiency loss due to shunting in perovskite/silicon tandem solar cells through modifying the resistive properties of the recombination junction. Sustainable Energy and Fuels, 2021, 5, 2036-2045.	4.9	10
349	A Blockchain-Supported Framework for Charging Management of Electric Vehicles. Energies, 2021, 14, 7144.	3.1	10
350	Study of CdTe/CdS solar cells using CSS CdTe deposited at low temperature. , 0, , .		9
351	Record fast thermal processing of 17.5Â efficient silicon solar cells. Semiconductor Science and Technology, 2002, 17, 677-681.	2.0	9
352	Microcrystalline Silicon Solar Cells: Theory and Diagnostic Tools. , 2006, , .		9
353	Proton-induced degradation of thin-film microcrystalline silicon solar cells. Journal of Non-Crystalline Solids, 2006, 352, 1851-1854.	3.1	9
354	Light Trapping effects in Thin Film Silicon Solar Cells. Materials Research Society Symposia Proceedings, 2009, 1153, 1.	0.1	9
355	Experimental Evaluation of the Light Trapping Potential of Optical Nanostructures for Thin-Film Silicon Solar Cells. Energy Procedia, 2012, 15, 206-211.	1.8	9
356	Light trapping in solar cells: numerical modeling with measured surface textures. Optics Express, 2015, 23, A539.	3.4	9
357	Simultaneous realization of light distribution and trapping in micromorph tandem solar cells using novel double-layered antireflection coatings. Solar Energy Materials and Solar Cells, 2015, 143, 546-552.	6.2	9
358	Advanced silicon thin films for high-efficiency silicon heterojunction-based solar cells. , 2017, , .		9
359	Optimized Design of Silicon Heterojunction Solar Cells for Field Operating Conditions. IEEE Journal of Photovoltaics, 2019, 9, 1541-1547.	2.5	9
360	Contributions to the Contact Resistivity in Fired Tunnel-Oxide Passivating Contacts for Crystalline Silicon Solar Cells. IEEE Journal of Photovoltaics, 2019, 9, 1548-1553.	2.5	9

#	Article	IF	CITATIONS
361	Influence of the Dopant Gas Precursor in P-Type Nanocrystalline Silicon Layers on the Performance of Front Junction Heterojunction Solar Cells. IEEE Journal of Photovoltaics, 2021, 11, 944-956.	2.5	9
362	In situ TEM observation of nickel promoted WS2 thin-film crystallization. Journal of Crystal Growth, 1998, 193, 109-113.	1.5	8
363	Impact of secondary gas-phase reactions on microcrystalline silicon solar cells deposited at high rate. Applied Physics Letters, 2010, 96, .	3.3	8
364	Amorphous silicon-based microchannel plates. Nuclear Instruments and Methods in Physics Research, Section A: Accelerators, Spectrometers, Detectors and Associated Equipment, 2012, 695, 74-77.	1.6	8
365	Current matching optimization in high-efficiency thin-film silicon tandem solar cells. , 2013, , .		8
366	Fast and Nondestructive Detection on the EVA Gel Content in Photovoltaic Modules by Optical Reflection. IEEE Journal of Photovoltaics, 2015, 5, 759-765.	2.5	8
367	Elemental distribution and charge collection at the nanoscale on perovskite solar cells. , 2016, , .		8
368	Nanocrystalline silicon oxide stacks for silicon heterojunction solar cells for hot climates. AIP Conference Proceedings, 2018, , .	0.4	8
369	Nitride layer screening as carrier-selective contacts for silicon heterojunction solar cells. AIP Conference Proceedings, 2018, , .	0.4	8
370	Performance Limitations and Analysis of Silicon Heterojunction Solar Cells Using Ultra-Thin MoO <sub>x</sub> Hole-Selective Contacts. IEEE Journal of Photovoltaics, 2021, 11, 1158-1166.	2.5	8
371	Localisation of front side passivating contacts for direct metallisation of high-efficiency c-Si solar cells. Solar Energy Materials and Solar Cells, 2022, 235, 111455.	6.2	8
372	Nanoscopic trigonal pyramidal crystallites in WS2â^'x sputtered thin films: a scanning tunnelling microscopy study of initial growth. Surface Science, 1996, 366, L703-L708.	1.9	7
373	Ultra-Light Amorphous Silicon Cell for Space Applications. , 2006, , .		7
374	Image Sensors Based on Thin-film on CMOS Technology: Additional Leakage Currents due to Vertical Integration of the a-Si:H Diodes. Materials Research Society Symposia Proceedings, 2006, 910, 3.	0.1	7
375	Periodic textures for enhanced current in thin film silicon solar cells. Materials Research Society Symposia Proceedings, 2008, 1101, 1.	0.1	7
376	Ultra-high quality surface passivation of crystalline silicon wafers in large area parallel plate reactor at 40ÂMHz. Thin Solid Films, 2009, 517, 6401-6404.	1.8	7
377	Optimization of the Asymmetric Intermediate Reflector Morphology for High Stabilized Efficiency Thin n-i-p Micromorph Solar Cells. IEEE Journal of Photovoltaics, 2013, 3, 41-45.	2.5	7
378	Large-area Hybrid Silicon Heterojunction Solar Cells with Ni/Cu Plated Front Contacts. Energy Procedia, 2014, 55, 715-723.	1.8	7

#	Article	IF	CITATIONS
379	Hole selective MoO <inf>x</inf> contact for silicon heterojunction solar cells. , 2014, , .		7
380	Scanning Laser-Beam-Induced Current Measurements of Lateral Transport Near-Junction Defects in Silicon Heterojunction Solar Cells. IEEE Journal of Photovoltaics, 2014, 4, 154-159.	2.5	7
381	Direct Imaging of Dopant Distribution in Polycrystalline ZnO Films. ACS Applied Materials & Interfaces, 2017, 9, 7241-7248.	8.0	7
382	Amorphous silicon-based micro-channel plate detectors with high multiplication gain. Nuclear Instruments and Methods in Physics Research, Section A: Accelerators, Spectrometers, Detectors and Associated Equipment, 2018, 912, 343-346.	1.6	7
383	Amorphous/Crystalline Silicon Interface Stability: Correlation between Infrared Spectroscopy and Electronic Passivation Properties. Advanced Materials Interfaces, 2020, 7, 2000957.	3.7	7
384	Evaluating Materials Design Parameters of Hole-Selective Contacts for Silicon Heterojunction Solar Cells. IEEE Journal of Photovoltaics, 2021, 11, 247-258.	2.5	7
385	Routing of Electric Vehicles With Intermediary Charging Stations: A Reinforcement Learning Approach. Frontiers in Big Data, 2021, 4, 586481.	2.9	7
386	Advanced method for electrical characterization of carrier-selective passivating contacts using transfer-length-method measurements under variable illumination. Journal of Applied Physics, 2021, 129, .	2.5	7
387	Input silane concentration effect on the a-Si:H to μc-Si:H transition width. Solar Energy Materials and Solar Cells, 2010, 94, 432-435.	6.2	6
388	Boosting the efficiency of III-V/Si tandem solar cells. , 2016, , .		6
389	Ultra-Lightweight PV module design for Building Integrated Photovoltaics. , 2017, , .		6
390	Automated Quantification of PV Hosting Capacity In Distribution Networks Under User-Defined Control and Optimisation Procedures. , 2018, , .		6
391	The amazing improvement of silicon heterojunction technology: ready for a true mass market launch. , 2018, , .		6
392	Characterization of Amorphous Silicon Based Microchannel Plates with High Aspect Ratio. , 2019, , .		6
393	Passivating Polysilicon Recombination Junctions for Crystalline Silicon Solar Cells. Physica Status Solidi - Rapid Research Letters, 2021, 15, 2100272.	2.4	6
394	Operating Temperatures and Diurnal Temperature Variations of Modules Installed in Open-Rack and Typical BIPV Configurations. IEEE Journal of Photovoltaics, 2022, 12, 133-140.	2.5	6
395	Longâ€Term Performance and Shade Detection in Building Integrated Photovoltaic Systems. Solar Rrl, 2022, 6, 2100583.	5.8	6
396	Transferability of the Light-Soaking Benefits on Silicon Heterojunction Cells to Module. IEEE Journal of Photovoltaics, 2022, 12, 662-668.	2.5	6

#	Article	IF	CITATIONS
397	Research and developments in thin-film silicon photovoltaics. , 2009, , .		5
398	Micro-Channel Plate Detectors Based on Hydrogenated Amorphous Silicon. Materials Research Society Symposia Proceedings, 2010, 1245, 1.	0.1	5
399	Microcrystalline and micromorph device improvements through combined plasma and material characterization techniques. Solar Energy Materials and Solar Cells, 2011, 95, 134-137.	6.2	5
400	Measurement of the Open-Circuit Voltage of Individual Subcells in a Dual-Junction Solar Cell. IEEE Journal of Photovoltaics, 2012, 2, 164-168.	2.5	5
401	Charge collection in amorphous silicon solar cells: Cell analysis and simulation of high-efficiency pin devices. Journal of Non-Crystalline Solids, 2012, 358, 2187-2189.	3.1	5
402	Super-Lambertian photocurrent-generation in solar cells with periodically textured interfaces. Applied Physics Letters, 2013, 103, 131108.	3.3	5
403	Thin-film limit formalism applied to surface defect absorption. Optics Express, 2014, 22, 31466.	3.4	5
404	Photolithography-free interdigitated back-contacted silicon heterojunction solar cells with efficiency >21%. , 2014, , .		5
405	High-performance hetero-junction crystalline silicon photovoltaic technology. , 2014, , .		5
406	Design of periodic nano- and macro-scale textures for high-performance thin-film multi-junction solar cells. Journal of Optics (United Kingdom), 2016, 18, 064005.	2.2	5
407	Optical Evaluation of the Rear Contacts of Crystalline Silicon Solar Cells by Coupled Electromagnetic and Statistical Ray-Optics Modeling. IEEE Journal of Photovoltaics, 2017, 7, 718-726.	2.5	5
408	Towards an optimum silicon heterojunction solar cell configuration for high temperature and high light intensity environment. Energy Procedia, 2017, 124, 331-337.	1.8	5
409	Analysis of lithium-ion cells performance, through novel test protocol for stationary applications. , 2017, , .		5
410	Reassessment of cell to module gains and losses: Accounting for the current boost specific to cells located on the edges. AIP Conference Proceedings, 2018, , .	0.4	5
411	Impact of the oxygen content on the optoelectronic properties of the indium-tin-oxide based transparent electrodes for silicon heterojunction solar cells. AIP Conference Proceedings, 2019, , .	0.4	5
412	Quantifying competitive grain overgrowth in polycrystalline ZnO thin films. Acta Materialia, 2019, 173, 74-86.	7.9	5
413	Effects of Work Function and Electron Affinity on the Performance of Carrier-Selective Contacts in Silicon Solar Cells Using ZnSn <sub>\$_ext{} x \$</sub> Ge <sub>\$_ext{} 1-x \$</sub> N\$_ext{2}\$ as a Case Study. IEEE Journal of Photovoltaics, 2021, 11, 1350-1357.	2.5	5
414	In Situ Reflectometry and Diffraction Investigation of the Multiscale Structure of p-Type Polysilicon Passivating Contacts for c-Si Solar Cells. ACS Applied Materials & Interfaces, 2022, , .	8.0	5

#	Article	IF	CITATIONS
415	Local series resistance mapping of silicon solar cells by microwave photoconductivity decay measurements. Progress in Photovoltaics: Research and Applications, 2003, 11, 309-317.	8.1	4
416	Boron Doping Effects on the Electro-optical Properties of Zinc Oxide Thin Films Deposited by Low-Pressure Chemical Vapor Deposition Process. Materials Research Society Symposia Proceedings, 2006, 928, 1.	0.1	4
417	Performance and Transient Behavior of Vertically Integrated Thin-film Silicon Sensors. Sensors, 2008, 8, 4656-4668.	3.8	4
418	Highâ€rate deposition of microcrystalline silicon in a largeâ€area PECVD reactor and integration in tandem solar cells. Progress in Photovoltaics: Research and Applications, 2010, 18, 257-264.	8.1	4
419	High-efficiency silicon heterojunction solar cells: From physics to production lines. , 2010, , .		4
420	Enhanced mobility of hydrogenated MO-LPCVD ZnO contacts for high performances thin film silicon solar cells. Materials Research Society Symposia Proceedings, 2012, 1426, 51-56.	0.1	4
421	High Spatial Resolution of Thin-Film-on-ASIC Particle Detectors. IEEE Transactions on Nuclear Science, 2012, 59, 2614-2621.	2.0	4
422	Ethanol-enriched low-pressure chemical vapor deposition ZnO bilayers: Properties and growth—A potential electrode for thin film solar cells. Journal of Applied Physics, 2013, 113, 024908.	2.5	4
423	Multi-occupancy buildings as micro-grids: an asset for integrating photovoltaics in power systems. , 2014, , .		4
424	The role of front and back electrodes in parasitic absorption in thin-film solar cells. EPJ Photovoltaics, 2014, 5, 50601.	1.6	4
425	The boron-tailing myth in hydrogenated amorphous silicon solar cells. Applied Physics Letters, 2015, 107, 201112.	3.3	4
426	Modeling of Voids Evolution in the Encapsulation Process of Photovoltaic Modules. Polymers and Polymer Composites, 2015, 23, 375-388.	1.9	4
427	Effect of Cooling Press on the Optical Transmission Through Photovoltaic Encapsulants. Polymer-Plastics Technology and Engineering, 2015, 54, 416-424.	1.9	4
428	Superhard, Antireflective Texturized Coatings Based on Hyperbranched Polymer Composite Hybrids for Thinâ€Film Solar Cell Encapsulation. Energy Technology, 2015, 3, 366-372.	3.8	4
429	Passivating contacts for silicon solar cells with 800 $\hat{A}^oC$ stability based on tunnel-oxide and highly crystalline thin silicon layer. , 2016, , .		4
430	MoOx and WOx based hole-selective contacts for wafer-based Si solar cells. , 2017, , .		4
431	Silicon Heterojunction Solar Cells on Quasi-mono Wafers. , 2018, , .		4
432	Gallium Nitride as Transparent Electron-Selective Contact in Silicon Heterojunction Solar Cells. , 2019, , .		4

#	Article	IF	CITATIONS
433	Impact of rapid thermal processing on bulk and surface recombination mechanisms in FZ silicon with fired passivating contacts. Solar Energy Materials and Solar Cells, 2022, 238, 111647.	6.2	4
434	Fracture mechanisms of GaAs under nanoscratching. Materials Research Society Symposia Proceedings, 2004, 841, R9.15.1.	0.1	3
435	Radiation hard amorphous silicon particle sensors. Materials Research Society Symposia Proceedings, 2005, 862, 1541.	0.1	3
436	Numerical Simulation of Microcrystalline Silicon Growth on Structured Substrate. Materials Research Society Symposia Proceedings, 2006, 910, 2.	0.1	3
437	Optical emission spectroscopy to diagnose powder formation in SiH 4 -H 2 discharges. , 2009, , .		3
438	Light scattering at nano-textured surfaces in thin film silicon solar cells. , 2010, , .		3
439	Enhanced light trapping in realistic thin film solar cells using one-dimensional gratings. Proceedings of SPIE, 2011, , .	0.8	3
440	A-Si:H/c-Si heterojunctions: a future mainstream technology for high-efficiency crystalline silicon solar cells?. , 2012, , .		3
441	Insights into the Encapsulation Process of Photovoltaic Modules: GC-MS Analysis on the Curing Step of Poly(ethylene-co-vinyl acetate) (EVA) Encapsulant. Polymers and Polymer Composites, 2012, 20, 665-672.	1.9	3
442	Anodic degradation of ZnO on soda-lime glass. Solar Energy Materials and Solar Cells, 2013, 117, 569-576.	6.2	3
443	Surface and Ultrathin-layer Absorptance Spectroscopy for Solar Cells. Energy Procedia, 2014, 60, 57-62.	1.8	3
444	Metal-free crystalline silicon solar cells in module. , 2015, , .		3
445	Facile preparation of micron- and nano-scale textured master for nano-imprinting front electrode in thin-film silicon tandem cells with improved light trapping. Solar Energy, 2015, 115, 518-524.	6.1	3
446	Alleviating power quality issues when integrating PV into built areas: Design and control of DC microgrids. , 2015, , .		3
447	New guidelines for a more accurate extraction of solar cells and modules key data from their current–voltage curves. Progress in Photovoltaics: Research and Applications, 2017, 25, 623-635.	8.1	3
448	Impact of organic overlayers on <i>a</i> -Si:H/ <i>c</i> -Si surface potential. Applied Physics Letters, 2017, 110, .	3.3	3
449	Notice of Removal Microcrystalline silicon carrier collectors for silicon heterojunction solar cells and impact on low-temperature device characteristics. , 2017, , .		3
450	Perovskite/Silicon Tandem Solar Cells: Challenges Towards High- Efficiency in 4-Terminal and		3

Monolithic Devices. , 2017, , .

#	Article	IF	CITATIONS
451	Injection-dependent lateral resistance in front-junction solar cells with nc-Si:H and a-Si:H hole selective contact. , 2019, , .		3
452	Influence of local surface defects on the minority-carrier lifetime of passivating-contact solar cells. Applied Physics Letters, 2020, 116, 113901.	3.3	3
453	Worldwide performance evaluation of ground surface reflectance models. Solar Energy, 2021, 224, 1063-1078.	6.1	3
454	Micro Photovoltaic Modules for Micro Systems. Materials Research Society Symposia Proceedings, 2008, 1066, 1.	0.1	2
455	A New Approach to Light Scattering from Nanotextured Interfaces For Silicon Thin-film Solar Cells. Materials Research Society Symposia Proceedings, 2010, 1245, 1.	0.1	2
456	Electrically flat/optically rough substrates for efficiencies above 10% in n-i-p thin-film silicon solar cells. Materials Research Society Symposia Proceedings, 2012, 1426, 39-44.	0.1	2
457	Light harvesting schemes for high efficiency thin film silicon solar cells. , 2012, , .		2
458	Optical properties of anodically degraded ZnO. Journal of Applied Physics, 2014, 115, 094902.	2.5	2
459	Resonant Absorption Enhancement in Solar Cells With Periodically Textured Interfaces. IEEE Journal of Photovoltaics, 2014, 4, 785-790.	2.5	2
460	High-efficiency perovskite/silicon heterojunction tandem solar cells. , 2016, , .		2
461	Modeling Potential-Induced Degradation (PID) of Field-Exposed Crystalline Silicon Solar PV Modules: Focus on a Regeneration Term. , 2017, , .		2
462	Mechanically stacked 4-terminal III-V/Si tandem solar cells. , 2017, , .		2
463	Direct Contact to TCO with SmartWire Connection Technology. , 2018, , .		2
464	Hybrid sequential deposition process for fully textured perovskite/silicon tandem solar cells. , 2018, ,		2
465	Numerical simulation of temperature dependence of MoOx based SHJ solar cell. AIP Conference Proceedings, 2018, , .	0.4	2
466	Monte Carlo Modeling of Electron Multiplication in Amorphous Silicon Based Microchannel Plates. , 2019, , .		2
467	A "combi-encapsulant" for enhanced performance of glass-free lightweight crystalline silicon solar PV modules. , 2021, , .		2
468	Monitoring the Operating Temperatures of Modules in Open-Rack and Typical BIPV Configurations. , 2021, , .		2

#	Article	IF	CITATIONS
469	Calibration of ground surface albedo models. Solar Energy, 2022, 237, 239-252.	6.1	2
470	Single photon detection with amorphous silicon-based microchannel plates: A Monte Carlo model. Nuclear Instruments and Methods in Physics Research, Section A: Accelerators, Spectrometers, Detectors and Associated Equipment, 2022, 1032, 166589.	1.6	2
471	Optical developments for silicon thin film solar cells in the substrate configuration. Materials Research Society Symposia Proceedings, 2008, 1101, 1.	0.1	1
472	Structural, optical, and electrical properties of silicon nanowires for solar cells. , 2010, , .		1
473	Conventional and 360 degree electron tomography of a micro-crystalline silicon solar cell. Journal of Physics: Conference Series, 2011, 326, 012057.	0.4	1
474	High rate deposition of microcrystalline silicon with silicon oxide doped layers: Highlighting the competing roles of both intrinsic and extrinsinc defects on the cells performances. , 2011, , .		1
475	Excitation of plasmon and guided-mode resonances in thin film silicon solar cells. Materials Research Society Symposia Proceedings, 2012, 1391, 24.	0.1	1
476	Stencil-nanopatterned back reflectors for thin-film amorphous silicon n-i-p solar cells. , 2012, , .		1
477	Advanced intermediate reflector layers for thin film silicon tandem solar cells. , 2013, , .		1
478	Amorphous silicon based betavoltaic devices. Materials Research Society Symposia Proceedings, 2013, 1536, 73-78.	0.1	1
479	Experimental measurement of lateral transport in the inversion layer of silicon heterojunction solar cells. , 2013, , .		1
480	Methods to evaluate the effect of water ingress: towards ultra-reliable PV modules. , 2013, , .		1
481	THIN-FILM SOLAR CELLS BASED ON AMORPHOUS AND MICROCRYSTALLINE SILICON. Series on Photoconversion of Solar Energy, 2014, , 139-207.	0.2	1
482	"Thin silicon solar cells: A path to 35% shockley-queisser limits", a DOE funded FPACE II project. , 2014, , .		1
483	Soiling and value of cleaning for low-tilt PV systems in temperate climates: a Swiss case study. , 2014, , $\cdot$		1
484	New concept of PECVD reactor for efficient production of silicon heterojunction solar cells. , 2015, , .		1
485	Advances in crystalline silicon heterojunction research and opportunities for low manufacturing costs. , 2015, , .		1
486	A scalable and inexpensive surface-texturization method for advanced transparent front electrodes in microcrystalline and micromorph thin film silicon solar cells. Physica Status Solidi (A) Applications and Materials Science, 2015, 212, 1916-1924.	1.8	1

#	Article	IF	CITATIONS
487	High performance amorphous Zn-Sn-O: impact of composition, microstructure, and thermal treatments in the optoelectronic properties. Proceedings of SPIE, 2017, , .	0.8	1
488	Improved ramp-rate and self consumption ratio in a renewable-energy-based DC micro-grid. , 2017, , .		1
489	Quantifying and Modeling the Impact of Interconnection Failures on the Electrical Performance of Crystalline Silicon Photovoltaic Modules. , 2018, , .		1
490	Engineering of Thin-Film Silicon Materials for High Efficiency Crystalline Silicon Solar Cells. , 2018, , .		1
491	Development of N-Type Amorphous and Microcrystalline Hydrogenated Silicon-Oxides (SiOx:H) and Investigation of their Impact as Window Layers on Silicon Heterojunction Solar Cells Device. , 2019, , .		1
492	Nanoscale Study of the Hole-Selective Passivating Contacts with High Thermal Budget Using C-AFM Tomography. ACS Applied Materials & Interfaces, 2021, 13, 9994-10000.	8.0	1
493	Potential Induced Degradation Mechanism in Rear-Emitter Bifacial Silicon Heterojunction Solar Cells Encapsulated in Different Module Structures. , 2021, , .		1
494	New Crystal Structures of WS2: Microtubes, Ribbons, and Ropes. , 1998, 10, 246.		1
495	Optimization of advanced surface-textures for thin-film silicon solar cells. , 2013, , .		1
496	PECVD based layers for improved high temperature industrial Solar cell processes. , 2019, , .		1
497	TEM characterization of textured silicon heterojunction solar cells. , 2008, , 335-336.		1
498	Bulk Defects and Hydrogenation Kinetics in Crystalline Silicon Solar Cells With Fired Passivating Contacts. IEEE Journal of Photovoltaics, 2022, 12, 711-721.	2.5	1
499	Bottom-Up and Top-Down Approaches for Identifying and Mitigating Electrical Losses in Silicon Heterojunction Solar Cells. IEEE Journal of Photovoltaics, 2022, 12, 906-914.	2.5	1
500	Characterization of a thick layer a-Si:H pixel detector with TFA technology using a scanning electron microscope. Journal of Non-Crystalline Solids, 2006, 352, 1832-1836.	3.1	0
501	Micromorph tandem solar cells grown at high rate with in-situ intermediate reflector in industrial KAI PECVD reactors. Conference Record of the IEEE Photovoltaic Specialists Conference, 2008, , .	0.0	0
502	Silane depletion dependent ion bombardment and material quality of microcrystalline silicon deposited by VHF-PECVD. Conference Record of the IEEE Photovoltaic Specialists Conference, 2008, , .	0.0	0
503	Conducting two-phase silicon oxide layers for thin-film silicon solar cells. Materials Research Society Symposia Proceedings, 2008, 1123, 9.	0.1	0

Laser-based plasma diagnostics for PECVD of silicon thin films. , 2009, , .

#	Article	IF	CITATIONS
505	Nanoscale Analysis by EFTEM and FIB-Tomography for Optimization of Thin-Film Silicon Solar Cells. Microscopy and Microanalysis, 2010, 16, 1336-1337.	0.4	0
506	UV-embossed textured back reflector structures for thin film silicon solar cells. Materials Research Society Symposia Proceedings, 2010, 1245, 1.	0.1	0
507	Back Cover: Optimization of thin film silicon solar cells on highly textured substrates (Phys. Status) Tj ETQq1 1 0.	784314 rg 1.8	gBT /Overlact
508	Enhancement of microcrystalline n-i-p solar cell performance via use of pre-covering layers and H2 treatment. Thin Solid Films, 2011, 519, 5567-5570.	1.8	0
509	Increasing short-circuit current in silicon heterojunction solar cells. , 2011, , .		0
510	Reflectance Improvement by Thermal Annealing of Sputtered Ag/ZnO Back Reflectors in a-Si:H Thin Film Silicon Solar Cells. Materials Research Society Symposia Proceedings, 2011, 1321, 63.	0.1	0
511	Amorphous Silicon Based Particle Detectors. Materials Research Society Symposia Proceedings, 2011, 1321, 423.	0.1	0
512	Model-based Quantitative Assessment of Crystallinity and Parasitic Absorption in Microcrystalline Silicon Solar Cells. Materials Research Society Symposia Proceedings, 2012, 1426, 383-387.	0.1	0
513	Innovative Device Architecture for High Efficiency Thin Film Silicon Solar Cells. Materials Research Society Symposia Proceedings, 2012, 1426, 131-135.	0.1	0
514	Optimization of the asymmetric intermediate reflector morphology for high stabilized efficiency thin n-i-p micromorph solar cells. , 2012, , .		0
515	Transparent conductive oxide / encapsulant interface characterization following Damp Heat exposure. , 2012, , .		0
516	On the interplay between microstructure and interfaces in high-efficiency microcrystalline silicon solar cells. , 2012, , .		0
517	Modulated Surface Textures for Enhanced Scattering in Thin-Film Silicon Solar Cells. , 2012, , .		0
518	Back Cover: Solar cell efficiency enhancement via light trapping in printable resonant dielectric nanosphere arrays (Phys. Status Solidi A 2/2013). Physica Status Solidi (A) Applications and Materials Science, 2013, 210, .	1.8	0
519	Nanomoulding of Functional Materials, a Versatile Complementary Pattern Replication Method to Nanoimprinting. Journal of Visualized Experiments, 2013, , .	0.3	0
520	Optimization of the asymmetric intermediate reflector morphology for high stabilized efficiency thin n-i-p micromorph solar cells. , 2013, , .		0
521	On the interplay between microstructure and interfaces in high-efficiency microcrystalline silicon solar cells. , 2013, , .		0
522	Post-deposition treatment of microcrystalline silicon solar cells for improved performance on rough superstrates. Journal of Applied Physics, 2014, 116, 244504.	2.5	0

#	Article	IF	CITATIONS
523	Parasitic absorption effects in metallic back reflectors with texture. , 2014, , .		Ο
524	Amorphous silicon/crystalline silicon heterojunction solar cells — Analysis of lateral conduction through the inversion layer. , 2014, , .		0
525	Silicon heterojunction solar cells with plated contacts for low to medium concentration photovoltaics. , 2015, , .		0
526	Transparent electrodes in silicon heterojunction solar cells: Influence on carrier recombination. , 2015, , .		0
527	Passivated interfaces in fluorinated microcrystalline silicon thin film solar cells. , 2015, , .		0
528	Absorption Enhancement in Solar Cells With Periodic Interface Textures of Asymmetric Shape. IEEE Journal of Photovoltaics, 2015, 5, 1534-1539.	2.5	0
529	Advanced TEM characterization of new electrical contacts for high efficiency c-Si solar cells. Microscopy and Microanalysis, 2016, 22, 1624-1625.	0.4	0
530	High Temperature Stability of Amorphous Zn-Sn-O Transparent Conductive Oxides Investigated by In Situ TEM and X-ray Diffraction. Microscopy and Microanalysis, 2016, 22, 1582-1583.	0.4	0
531	Exploring silicon carbide- and silicon oxide-based layer stacks for passivating contacts to silicon solar cells. , 2017, , .		0
532	A passivating contact concept compatible with a short thermal treatment. , 2018, , .		0
533	Corrections to "Highly Conductive and Broadband Transparent Zr-Doped In2O3 as Front Electrode for Solar Cells―[Sep 18 1202-1207]. IEEE Journal of Photovoltaics, 2019, 9, 1155-1155.	2.5	0
534	Efficient semitransparent perovskite minimodule with highly transparent and conductive multilayer electrode. , 0, , .		0
535	ZnSnxGe1-xN2 as electron-selective contact for silicon heterojunction solar cells. , 2021, , .		0
536	EVA for Glass/Glass Solar PV Modules: Effect of encasulant storage conditions and process parameters. , 2021, , .		0
537	Photocurrent Increase in Thin Film Solar Cells by Guided Mode Excitation. , 2010, , .		0
538	An RCWA Analysis of Solar Cell Back Reflectors: Comparison between Modelling and Experiment. , 2010, , .		0
539	A New Approach to Light Scattering from Nanotextured Interfaces for Silicon Thin-Film Solar Cells. , 2010, , .		0
540	Advanced nanostructured materials for pushing light trapping towards the Yablonovitch limit. , 2011,		0

#	Article	IF	CITATIONS
541	Light Trapping Limit Revisited: How do Guided Modes Enhance Light Absorption in Solar Cells?. , 2012, , .		0
542	Geometrical Impact on Guided Mode Excitation in Solar Cells. , 2012, , .		0
543	Coupling between radiation and internal modes: light trapping in thin film solar cells with periodic texture. , 2012, , .		0
544	Light-trapping in the near field: the case for plasmonic thin-film solar cells. , 2013, , .		0
545	Multifunctional Antireflection Coatings for High-Efficient Light Harvesting in Photovoltaic Devices. , 2016, , .		0
546	Photoinduced Halide Segregation and Diffusion in Mixed-halide Perovskite Solar Cells. , 0, , .		0
547	Stability of perovskite and two terminal Si/perovskite tandem solar cells under reverse bias. , 0, , .		0
548	A nanometric view on performance-loss mechanisms in perovskite/c-Si multi-junction solar cells. , 0, , .		0
549	Quantitative Analysis of Nanorough Hydrogenated Si(111) Surfaces through Vibrational Spectral Assignment by Periodic DFT Calculations. Journal of Physical Chemistry C, 2022, 126, 8278-8286.	3.1	0
550	Degradation due to Transverse Ion Migration in Perovskite Devices. , 0, , .		0